[CANCER RESEARCH 62, 3636–3640, July 1, 2002]

Advances in Brief

Genomic Copy Number Analysis of Non-small Cell Lung Cancer Using Array Comparative Genomic Hybridization: Implications of the Phosphatidylinositol 3-Kinase Pathway[1]

Pierre P. Massion, Wen-Lin Kuo, David Stokoe, Adam B. Olshen, Patrick A. Treseler, Koei Chin, Chira Chen, Daniel Polikoff, Ajay N. Jain, Daniel Pinkel, Donna G. Albertson, David M. Jablons, and Joe W. Gray[2]

UCSF Comprehensive Cancer Center [P. P. M., W. L. K., A. B. O., K. C., C. C., D. Po.], Cancer Research Institute [D. S., D. A.], Department of Laboratory Medicine [D. Pi., J. W. G.], Department of Surgery [D. J.], and Department of Pathology [P. A. T.], University of California, San Francisco, California 94143

Abstract

Genomic abnormalities at 348 loci encoding genes that may contribute to lung cancer transformation and progression were assessed using array comparative genomic hybridization in 21 squamous carcinomas (SqCas) and 16 adenocarcinomas (AdCas). Hierarchical clustering showed a clear pattern of gains and losses for the SqCas, whereas the pattern for AdCas was less distinct. Cross-validated classification using a *K*-nearest-neighbor assigned, on average, 32 of 37 samples to their proper histological subtype. The most noticeable differences between SqCas and AdCas were gain of chromosome 3q22-q26 and loss of chromosome 3p. These occurred almost exclusively in SqCas. The region of recurrent increase is ~30 Mb in extent, ranging from *EVI1* to *TFRC*. *PIK3CA*, the α catalytic subunit of phosphatidylinositol 3-kinase (PI3K), is in this region. The *PIK3CA* copy number increase was validated using fluorescence *in situ* hybridization to lung cancer tissue microarrays. Activity of the downstream PI3K effector protein kinase B (*PKB*) was higher in SqCas than in AdCas and was correlated with *PIK3CA* copy number ($r = 0.75$), suggesting that these copy number increases contribute to activation of PI3K signaling in SqCas of the lung.

Introduction

Lung cancer is the most common cause of cancer death in North America. NSCLC[3] represents approximately 75% of all lung cancers, 80% of which are classified as SqCa or AdCa. At present, the treatment and the prognosis of these two subtypes are similar, and they share genetic characteristics such as degree of aneuploidy (1) and prevalence of microsatellite instability (2). However, the two histological subtypes also appear as different diseases at both the pathological and molecular level. For example, *K-ras* and *p53* mutations are more frequent in AdCas than in SqCas, and AdCas have a lower frequency of loss of heterozygosity (3). CGH analyses, on the other hand, show that amplification of chromosome 3q25-qter is more frequent in SqCas (4–6). Several candidate genes that could play an important role in the pathogenesis of SqCas of the lung have been identified in this region of amplification, among them the α catalytic subunit PI3K (*PIK3CA*) (6, 7). This is of interest because several cancer-related functions have been associated with increased PI3K signaling, and aberrations involving the PI3K pathway genes *PIK3CA*, *PKB*, and *PTEN* have been implicated in several cancer types including lung cancer (8). These studies motivated the present study of genome copy number abnormalities involving these and other receptor tyrosine kinase signaling pathway genes in NSCLC SqCas and AdCas. We accomplished this by applying array CGH to analysis of relative copy number at 348 known or suspected cancer genes including several elements of the PI3K signaling pathway. We also assessed the extent to which *PIK3CA* copy number increases were correlated with activation of the downstream PI3K effector, *PKB*.

Materials and Methods

CGH. Twenty-one SqCas and 16 AdCas of the lung were selected for array CGH analysis from archival tissue at the University of California San Francisco. Tumor DNA was extracted from paraffin-embedded formalin-fixed 30-μm sections. Microdissected samples containing at least 75% cancer cells were deparaffinized with xylene and ethanol, digested with proteinase K, and purified by phenol-chloroform extraction. The DNA samples were then resuspended in water and digested with *Dpn*II. One μg of each tumor DNA sample was labeled with CY3 by random priming (Bioprime random priming kit) to incorporate Cy3-dUTP. Simultaneously, and for every experiment, normal sex-matched human DNA was labeled with CY5-dUTP to provide a reference probe.

Briefly, DNA samples from 348 BAC clones carrying genes of potential importance in cancer genesis or progression were PCR-amplified using a degenerate oligonucleotide primer containing a 5′ amine group, printed in quadruplicate, and covalently attached to 3D-Link-activated slides (Surmodics Inc.).

Clones on the array are listed online.[4] Array CGH hybridizations were carried out as described elsewhere (9). Approximately 500 ng of each test and reference probe were coprecipitated with 50 μg of human Cot-1 DNA (Life Technologies, Inc.) and resuspended in 20 μl of hybridization mix (50% formamide, 10% dextran sulfate, 2× SSC, and 2% SDS). Probes were denatured at 72°C for 7 min, incubated at 37°C for 45 min, applied to the array slide inside a rubber cement dam, and incubated at 37°C in a humidified chamber (50% formamide, 2× SSC) on a rocker for 48–72 h. Slides were washed for 15 min at 48°C in 50% formamide and 2× SSC (pH 7.0), washed for 15 min at 48°C in 2× SSC and 0.1%SDS, and finally washed for 15 min at room temperature in PN buffer [0.1 M sodium phosphate buffer and 0.1% NP40 (pH 8.0)]. The slides were mounted with DAPI counterstain (0.5 mM DAPI, 0.1× PBS, and 90% glycerol) for imaging. A control normal male *versus* normal female array CGH hybridization was performed to confirm the ability on each hybridization day to detect the copy number difference on the X chromosome. Sixteen-bit TIF images were collected using a charge-coupled device camera through CY3, CY5, and DAPI filters and analyzed using GenePix software (Axon Inc.). CY3:CY5 ratios were calculated after background subtraction. Hybridization signals for each array element were accepted for analysis only if the correlation of the CY3 *versus* CY5 pixel intensities was >0.81, the number

Received 1/23/02; accepted 5/7/02.

The costs of publication of this article were defrayed in part by the payment of page charges. This article must therefore be hereby marked *advertisement* in accordance with 18 U.S.C. Section 1734 solely to indicate this fact.

[1] Research support was from USPHS Grant CA64602. P. P. M. was supported by a Parker B. Francis Fellowship and by a Research Grant from the American Lung Association.

[2] To whom requests for reprints should be addressed, at Cancer Genetics Program, University of California San Francisco, Comprehensive Cancer Center, 2340 Sutter Street, San Francisco, CA 94143-0808. Phone: (415) 476-3476; Fax: (415) 476-4228; E-mail: jgray@cc.ucsf.edu.

[3] The abbreviations used are: NSCLC, non-small cell lung cancer; CGH, comparative genomic hybridization; SqCa, squamous carcinoma; AdCa, adenocarcinoma; FISH, fluorescence *in situ* hybridization; PI3K, phosphatidylinositol 3-kinase; PKB, protein kinase B; BAC, bacterial artificial chromosome; DAPI, 4′,6-diamidino-2-phenylindole; KNN, *K*-nearest-neighbor.

[4] http://cc.ucsf.edu/gray/public.

of pixels was ≥40, and CY3 and CY5 intensities exceeded predetermined thresholds. Fluorescence ratios were normalized so that the mean of the middle third of ratios across the array was 1. Average ratios deviating significantly ($>3\sigma$) from 1 were considered abnormal.

NSCLC Tissue Microarrays. Tissue microarrays (10) were prepared from paraffin blocks for 69 SqCas and 90 AdCas of the lung (stage I-III) and from an equal number of normal lung tissues. Samples were archived at Moffitt Hospital and University of California San Francisco-Mount Zion Medical Center between 1989 and 2000. H&E-stained sections for all tissue blocks were reviewed by P. A. T. and P. P. M., and areas to be cored for array production were selected with marking ink. Small tumors were not included to leave material for patient care. Cores 0.6 mm in diameter were taken from the selected area of each specimen and inserted into a recipient paraffin block. Five-μm sections were cut from the arrays and mounted onto charged slides. Every 15th section was stained with H&E to confirm the continued presence of the histological feature of interest (cancer or normal). Tissue arrays were characterized by morphological examination, histochemical staining for mucicarmine, and immunostaining for cytokeratins 7 and 20 and common cancer-related proteins including p53, Bcl2, and Ki-67 to confirm published findings.

FISH. BAC and P1 clones for specific genes were selected from different libraries [*PIK3CA* (CTC-364E3), *PIK3CB* (CTB-138N2) and *AKT2* (CTB-166E20), *RhoA* (RP4-690P14), and a clone on 19p (P1–346F10)]. Interphase nuclei were stained using dual-color FISH. Briefly, 2 μg of BAC DNA were labeled by nick-translation with either digoxigenin-dUTP or Cy3-dUTP. Labeled probes were separated from the reaction using spin columns and denatured. Tissue sections were deparaffinized, dehydrated in 100% ethanol, treated with sodium thiocyanate for 10 min followed by pepsin (4 mg/ml) digestion in 0.2 N HCl for 10 min at 37°C, washed with water, and dehydrated with a graded ethanol series. Slides were then denatured in 70% formamide/2× SSC for 5 min at 72°C, dehydrated in graded ethanol, and incubated with a hybridization mixture consisting of 50% formamide, 2× SSC, Cot-1 DNA, and 100 ng of both digoxigenin-labeled and Cy3-labeled BAC DNAs. After ~48 h of incubation at 37°C, the slides were washed at 45°C in 50% formamide/2× SSC for 10 min and counterstained with antifade solution containing DAPI. Test and reference hybridization signals were scored in ~50 nuclei for each tumor core under a ×63 immersion objective. Nuclei in which the nuclear boundaries were broken were excluded from the analysis. The ratio of the mean count for the test probe to the mean count for the reference probe on the opposite chromosome arm was reported as the relative copy number for the test gene.

***PKB* Activity Assay.** Analysis for endogenous *PKB* activity was performed as described previously (11). Briefly, whole-cell lysates were prepared from 20–50 mg of lung tissue (tumor or normal lung) in 5 volumes of lysis buffer [1% NP40, 150 mM NaCl, 20 mM Tris (pH 7.5), 1 mM EDTA, 1 mM EGTA, 1 mM DTT, 1 mM $NaVO_4$, and 1 tablet of protease inhibitor mixture/10 ml lysis buffer (Boehringer Mannheim)]. After incubation on ice for 10 min, lysates were spun for 10 min at maximum speed in a microcentrifuge. Equal amounts of total protein from NSCLC tumor lysates and normal tissue were subjected to immunoprecipitation with *PKB* antibodies. The washed immune complex was incubated with 50 mM peptide substrate Crosstide (GRPRTSSFAEG), 5 mM $MgCl_2$, 20 mM ATP, and 5 mCi of [γ-^{32}P]ATP in a volume of 10 ml for 15 min at 30°C. The reaction was terminated by adding an equal volume of 2× Tricine loading gel buffer, and the phosphorylated peptide was separated from free [γ-^{32}P]ATP by electrophoresis on 16% Tricine gels (Novex).

Statistical Analysis. Statistical analyses focused on identification of genomic differences between SqCas and AdCas detected using array CGH. All CGH ratios were converted to log base 2, and array elements were eliminated if there were <10 successful relative copy number measurements in either tumor class. The resulting data set contained measurements for 348 loci. The difference in copy number between SqCas and AdCas for each locus was assessed by computing a two-sample *t* statistic with equal variances. Because of the multiple comparisons problem resulting from performing 348 tests, the *P* for each test was determined using a permutation-based method (12). The permutation procedure was as follows: (*a*) we permuted the class labels corresponding to each sample; and (*b*) we found the maximum absolute *t* statistic for the permuted data. This procedure was repeated 10,000 times. The *P* for each clone was computed as the proportion of permutations for which the maximum absolute *t* statistic was greater than the observed *t* statistic for the clone. Clones with $P < 0.05$ were termed "significant."

Agglomerative hierarchical clustering via single linkage with scaled Euclidean distance (all vectors are scaled to unit length) as the distance metric was used to examine similarity in samples across array elements (13). Only the 100 clones that were most significantly different between SqCas and AdCas were chosen for the distance computations. Formal prediction of samples as being AdCa or SqCa based on array data was conducted using KNN classification (14). The KNN classifier predicts the class for a sample based on a vote of the classes of its nearest neighbors. The parameter *K* stands for the number of nearest neighbors used in the vote. The scaled Euclidean distance was used to calculate the distances between samples. Because the sample size of the data set prohibited a split into a training and test set, repeated cross-validation was used to estimate the classification rate. The algorithm was as follows: (*a*) we split the data into 10 groups of nearly equal size; (*b*) we selected one group to be the test set and the other nine groups to be the training set; (*c*) we found the best number of genes and value for *K* in terms of classifying the training set; (*d*) we used the parameters determined in step *c* to predict the classes of the current test set; (*e*) we repeated steps *a*−*d* with each of the nine other groups successively serving as the test set; and (*f*) we repeated steps *a*−*e* 100 times and averaged the results. The optimal values for step *c* were determined using a nested cross-validation on just the training set. One final analysis compared log copy number to a set of covariates. The level of associated was determined using either the two-sample *t* statistic with equal variances or the Pearson correlation

Results and Discussion

Twenty-one SqCa and 16 AdCa NSCLCs and several normal samples were analyzed using array CGH. A typical normal male *versus* normal female analysis is shown in Fig. 1*A*. The CGH ratios are clearly reduced for X chromosome array elements, demonstrating the ability of array CGH to detect single copy number changes. A typical analysis of a SqCa is shown in Fig. 1*B*. Copy number gains involving several genes such as *PIK3CA* on 3q and *CCND1* on 11q are clearly visible. Frequency distributions showing recurrent gains and losses for the 21 SqCa and 16 AdCa NSCLCs, respectively, are presented in Fig. 2, *A* and *B*. In general, the number of abnormalities was substantially higher for SqCas than for AdCas. Cluster analysis using the 100 most informative array elements allowed accurate discrimination between SqCas and AdCas. KNN classification was used to formally test the ability to predict subtype from array CGH profile. Cross-validation yielded 32 of 37 (87%) correct histological classifications, on average (see "Materials and Methods"). Six of 348 analysis elements were significantly different between SqCas and AdCas using a permutation *t* test. The involved genes included (in descending order of statistical significance) *FHIT*, *PIK3CA*, *SST*, *TGFA*, and *GLUT2*, all in regions of gain or loss on chromosome 3. We found a possible relationship between genes amplified on chromosome 3q and genes deleted on chromosome 3p in SqCa. There were no pairwise comparisons that were significant using Fisher's exact test after adjusting for multiple comparisons, which was not surprising, given the limited sample size. However, of the 1176 pairwise comparisons, 126 (10.8%) had Ps < 0.05. This is significantly more than the 5% one would expect if the tests were independent and if there were no relationship. In particular, *FHIT*, *EG9F2*, and *CACNA1D* deletions were associated with amplification of *GLUT2*, *THRB*, *PIK3CA*, and *BCL6* in 50–65% of the SqCas.

Taken together, these results clearly demonstrate substantial molecular differences between SqCas and AdCas and are consistent with earlier chromosome-based CGH studies (4–6). The significant difference in the total number of abnormalities between SqCas and AdCas suggests that they may differ in the level of genome instability and/or in the mechanisms by which they pro-

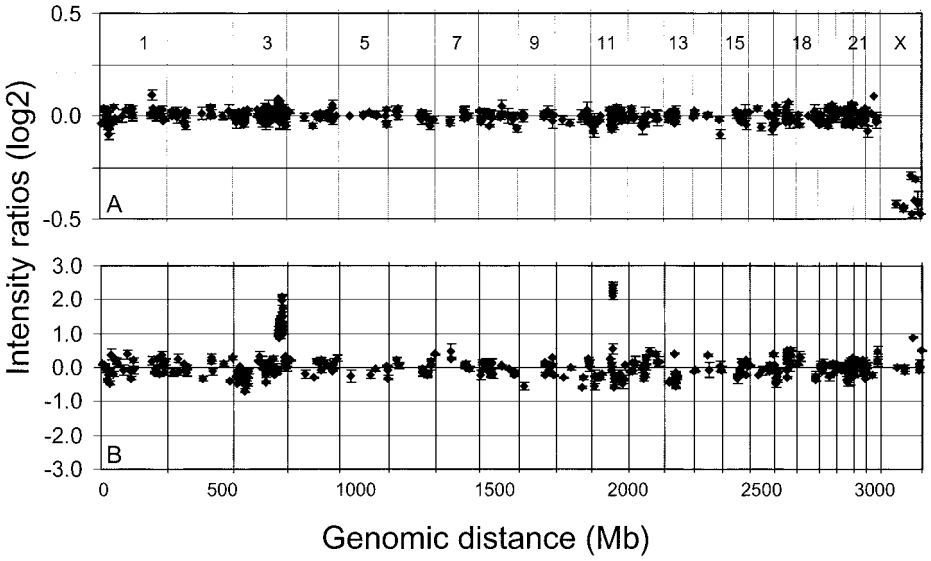

Fig. 1. Array CGH analyses. *A*, array CGH analysis of a normal male sample against a normal female reference. Each data point is presented as mean ($n = 4$) ± coefficient of variation (coefficient of variation = SD/mean). *B*, array CGH analysis of a SqCa of the lung tested against normal DNA. Each data point is presented as mean ($n = 4$) ± coefficient of variation (coefficient of variation = SD/mean). Chromosomal boundaries are indicated by *vertical lines*.

gress. These differences also suggest that different therapeutic approaches may be needed for these lung cancer subtypes.

Identification of the involved genes provides important information about the mechanisms by which tumor progress and may suggest approaches to gene-targeted therapy. Genes in regions of recurrent abnormality are initial candidates. Those increased in relative copy number (as defined by normalized intensity ratio >1.42) in >15% of the SqCas included *TGFA* (chromosome 2p); *SST*, *PIK3CA*, *BCL6*, *GLUT2*, *TERC*, *EVI1*, *AGTR*, *S1B11/PRLL*, and *TERF* (all at chromosome 3q); *ETO* (chromosome 8q); *FACC* (chromosome 9q22); *INT2*, *PCLB3*, and *CCND1* (chromosome 11q); *PRKCH* (chromosome 14q); *ERBB2* (chromosome 17q); and *JUNB* (chromosome 19p). Genes decreased in relative copy number in >15% of the SqCa tumors included *TGFBR3*, *EPHB2*, and *FRG* (chromosome 1p); *FHIT*, *THRB*, and *RHOA* (chromosome 3p); *ADRA1C* (chromosome 8p); *CDK14* (chromosome 9p); *PRKCB1* (chromosome 13q); and *SRC* (chromosome 20q). Copy number increase at 3q26 was the most frequent abnormality. The frequency with which genes in this region were present at increased copy number is shown in Fig. 3. Two maxima appear, one centered on *PIK3CA*, and the other centered on *SST*. Higher-resolution arrays may reveal other candidates in these and other regions of the genome.

Genes involved in PI3K signaling were of special interest because of the roles they play in activation of cell proliferation, cell migration, cell motility, and decrease of cell death in human tumors (for review, see Ref. 15). Because *PIK3CA*, encoding the p110α catalytic subunit of PI3K (16), was in a region of frequent copy number increase in SqCas and has been previously implicated in SqCa lung cancer (17), we assessed copy number at several PI3K pathway genes including *PIK3CA*, *PIK3CB*, *PIK3R1*, and *AKT2* in 68 SqCa and 90 AdCa NSCLCs arranged in tissue microarrays. We obtained FISH data on 53 of 68 tumors represented on the SqCa array and 62 of 90 tumors represented on the AdCa array. Missing biopsy samples on the slide and hybridization failures explain the absence of FISH data for the remaining tumors. In SqCas, relative copy number >2 was present in 31 of 52 tumors for *PIK3CA*, in 26 of 46 tumors for *PIK3CB*, and in 5 of 53 tumors for *AKT2*. In contrast, none of the 61 AdCa samples showed a copy number ratio > 2 for either *PIK3CA* or *PIK3CB*, and only 4 of 62 tumors showed a copy number ratio >2 for *AKT2*. Increased relative copy number *PIK3CA* did not correlate with gain of *PIK3CB* and/or *AKT2* ($r = 0.045$ and 0.012, respectively).

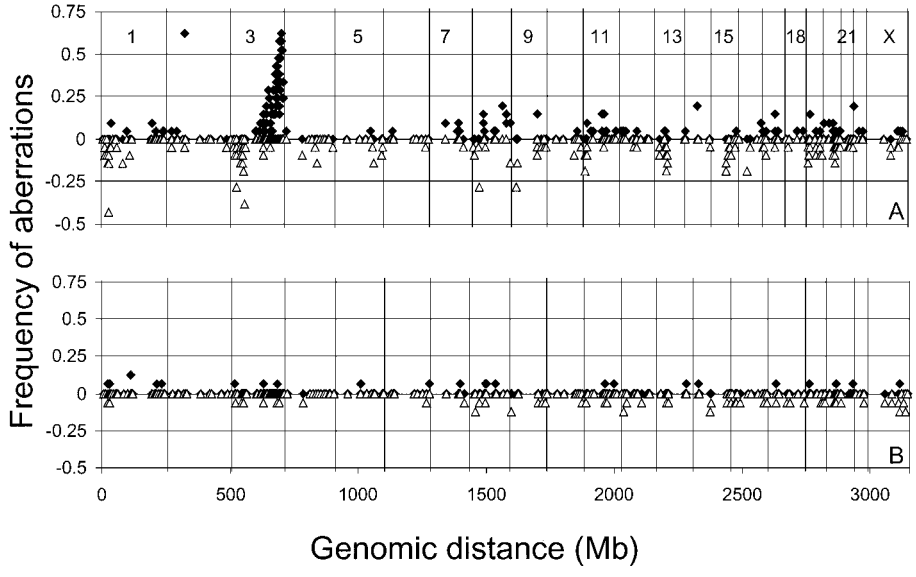

Fig. 2. Frequency of gene copy number abnormalities in NSCLC. *A*, frequencies of genes increased in copy number (normalized intensity ratios ≥1.5, ◆) or decreased in copy number (normalized intensity ratios ≤0.7, △) in SqCa of the lung. *B*, frequency of gene copy number abnormalities in AdCas of the lung. Chromosomal boundaries are indicated by *vertical lines*.

PIK3R1 on chromosome 5q13 was not increased in copy number in either SqCas or AdCas of the lung (data not shown).

The frequent copy number increase of *PIK3CA* in SqCas and its presence as the most highly amplified gene on the array in several tumors suggested that this event might up-regulate PI3K signaling in this subtype of NSCLC. We tested this possibility by measuring *PKB/AKT* activity in 10 SqCa and 6 AdCa samples. Fig. 4*A* shows that *PKB* activity was increased in SqCas as compared with AdCas. Fig. 4, *B* and *C*, shows that *PKB* activity was higher in SqCas with increased *PIK3CA* copy number than in those with normal *PIK3CA* copy number and that copy number of *PIK3CA* was correlated with *PKB* activity in SqCas ($r = 0.75$). *PIK3CB* copy number was not correlated with *PKB* activity (data not shown). In addition, the copy number changes did not correlate with other characteristics of the tumors including p53 and Bcl2 expression (antiapoptosis markers) and Ki-67 nuclear staining (proliferation index). These data indicate that the *PIK3CA* copy number increase does increase PI3K signaling in NSCLC SqCas and suggests the possibility that these tumors may be susceptible to PI3K inhibitors.

PIK3CA, of course, is unlikely to be the only gene important in lung cancer that is deregulated by copy number increase at 3q. The most frequent region of increase extends over ~30 Mb from *EVI1* to *TERF* and encodes several candidate genes. Somatostatin (*SST*) is of interest because it is located at the point of most frequent amplification on the array (Fig. 3). *SST* is a ligand for high-affinity cell surface receptors and is involved in endocrine function. Overexpression of the *EVI1* gene is associated with myeloid leukemia/myelodysplastic syndrome in both mouse and humans and has been implicated in ovarian cancer.[4] *SNO/SKIL* is important as a regulator of *TGFB* signaling (18). The zinc finger transcriptional repressor *BCL6* has been suggested as a proto-oncogene in diffuse large cell lymphoma (19). *TERC* encodes the RNA component of telomerase that acts as a template for the addition of telomeric repeat sequences (20). Although interesting, additional studies will be needed to determine whether the 3q copy number increase activates these genes and how this amplicon contributes to lung cancer development or progression.

In summary, we have shown that although SqCas and AdCas have a very similar outcome, these two diseases present with very distinct genomic profiles. *PIK3CA* was implicated as one possible oncogene whose amplification plays a role in NSCLC SqCa progression. Markers that reveal 3q26-28 amplification may be useful for SqCa detection. New antiproliferative strategies being developed to inhibit PI3K signal transduction may be particularly effective against SqCas.

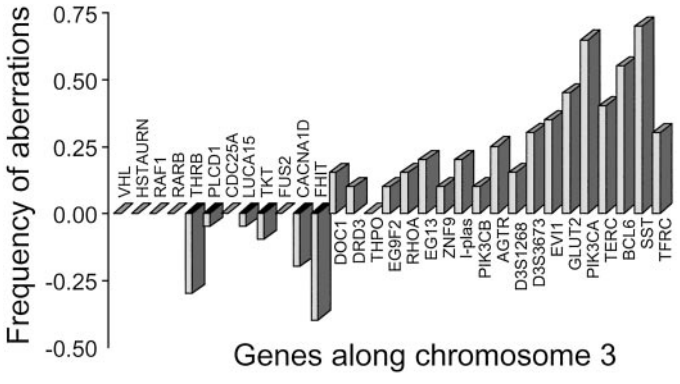

Fig. 3. Frequency of gene copy number abnormalities along chromosome 3 in 21 SqCas of the lung. Specific genes tested are shown along the *X* axis.

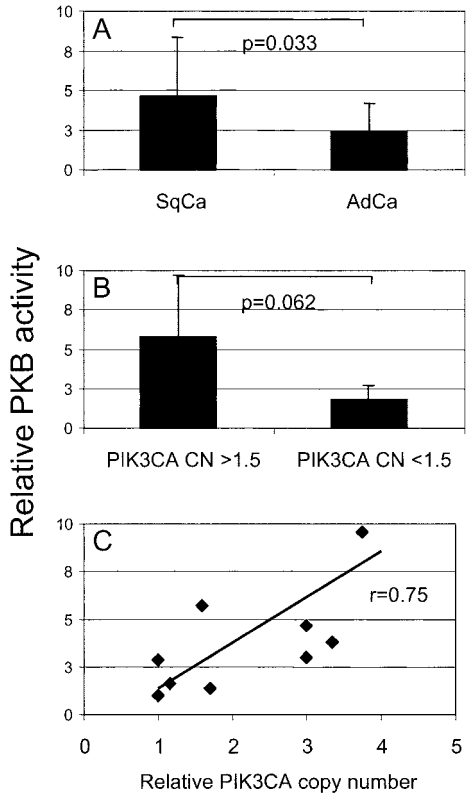

Fig. 4. *PKB* activity in SqCas and AdCas of the lung. *PKB* activity is expressed as the mean ± SD after normalization of the absolute value to the mean of the values. SqCas ($n = 10$) showed elevated *PKB* activity as compared with AdCas ($n = 6$) of the lung (*A*). We also found an increase in *PKB* activity among tumors with elevated *PIK3CA* copy number (≥1.5; $n = 7$) as compared with tumors with lower *PIK3CA* (≤1.5; $n = 3$; *B*). Values are mean ± SD; *P*s indicate differences tested by unpaired *t* test. Correlation between relative copy number of *PIK3CA* and *PKB* activity was found among SqCas of the lung (*C*).

Acknowledgments

We thank J. Basas and L. Riedell for excellent technical assistance for tissue array fabrication and FISH spot counting, respectively. We thank Norma Nowak and Jeffrey Conroy for the RP11 clones.

References

1. Taguchi, T., Zhou, J. Y., Feder, M., Litwin, S., Klein-Szanto, A. J., and Testa, J. R. Detection of aneuploidy in interphase nuclei from non-small cell lung carcinomas by fluorescence *in situ* hybridization using chromosome-specific repetitive DNA probes. Cancer Genet. Cytogenet., *89:* 120–125, 1996.
2. Wistuba, I. I., Behrens, C., Milchgrub, S., Bryant, D., Hung, J., Minna, J. D., and Gazdar, A. F. Sequential molecular abnormalities are involved in the multistage development of squamous cell lung carcinoma. Oncogene, *18:* 643–650, 1999.
3. Sato, S., Nakamura, Y., and Tsuchiya, E. Difference of allelotype between squamous cell carcinoma and adenocarcinoma of the lung. Cancer Res., *54:* 5652–5655, 1994.
4. Balsara, B. R., Sonoda, G., du Manoir, S., Siegfried, J. M., Gabrielson, E., and Testa, J. R. Comparative genomic hybridization analysis detects frequent, often high-level, overrepresentation of DNA sequences at 3q, 5p, 7p, and 8q in human non-small cell lung carcinomas. Cancer Res., *57:* 2116–2120, 1997.
5. Petersen, I., Bujard, M., Petersen, S., Wolf, G., Goeze, A., Schwendel, A., Langreck, H., Gellert, K., Reichel, M., Just, K., du Manoir, S., Cremer, T., Dietel, M., and Ried, T. Patterns of chromosomal imbalances in adenocarcinoma and squamous cell carcinoma of the lung. Cancer Res., *57:* 2331–2335, 1997.
6. Bjorkqvist, A. M., Husgafvel-Pursiainen, K., Anttila, S., Karjalainen, A., Tammilehto, L., Mattson, K., Vainio, H., and Knuutila, S. DNA gains in 3q occur frequently in squamous cell carcinoma of the lung, but not in adenocarcinoma. Genes Chromosomes Cancer, *22:* 79–82, 1998.
7. Racz, A., Brass, N., Heckel, D., Pahl, S., Remberger, K., and Meese, E. Expression analysis of genes at 3q26–q27 involved in frequent amplification in squamous cell lung carcinoma. Eur. J. Cancer, *35:* 641–646, 1999.
8. Moore, S. M., Rintoul, R. C., Walker, T. R., Chilvers, E. R., Haslett, C., and Sethi, T. The presence of a constitutively active phosphoinositide 3-kinase in small cell lung cancer cells mediates anchorage-independent proliferation via a protein kinase B and p70s6k-dependent pathway. Cancer Res., *58:* 5239–5247, 1998.

9. Pinkel, D., Segraves, R., Sudar, D., Clark, S., Poole, I., Kowbel, D., Collins, C., Kuo, W. L., Chen, C., Zhai, Y., Dairkee, S. H., Ljung, B. M., Gray, J. W., and Albertson, D. G. High resolution analysis of DNA copy number variation using comparative genomic hybridization to microarrays. Nat. Genet., *20:* 207–211, 1998.
10. Bubendorf, L., Kononen, J., Koivisto, P., Schraml, P., Moch, H., Gasser, T. C., Willi, N., Mihatsch, M. J., Sauter, G., and Kallioniemi, O. P. Survey of gene amplifications during prostate cancer progression by high-throughout fluorescence *in situ* hybridization on tissue microarrays [published erratum appears in Cancer Res., *59:* 1388, 1999]. Cancer Res., *59:* 803–806, 1999.
11. Stokoe, D., Stephens, L. R., Copeland, T., Gaffney, P. R., Reese, C. B., Painter, G. F., Holmes, A. B., McCormick, F., and Hawkins, P. T. Dual role of phosphatidylinositol-3,4,5-trisphosphate in the activation of protein kinase B. Science (Wash. DC), *277:* 567–570, 1997.
12. Jain, A. N., Chin, K., Borresen-Dale, A. L., Erikstein, B. K., Eynstein Lonning, P., Kaaresen, R., and Gray, J. W. Quantitative analysis of chromosomal CGH in human breast tumors associates copy number abnormalities with p53 status and patient survival. Proc. Natl. Acad. Sci. USA, *98:* 7952–7957, 2001.
13. Eisen, M. B., Spellman, P. T., Brown, P. O., and Botstein, D. Cluster analysis and display of genome-wide expression patterns. Proc. Natl. Acad. Sci. USA, *95:* 14863–14868, 1998.
14. Duda, R. O., and Hart, P. E. Pattern Classification and Scene Analysis. New York: John Wiley & Sons, 1973.
15. Krasilnikov, M. A. Phosphatidylinositol-3 kinase dependent pathways: the role in control of cell growth, survival, and malignant transformation. Biochemistry (Mosc.), *65:* 59–67, 2000.
16. Hiles, I. D., Otsu, M., Volinia, S., Fry, M. J., Gout, I., Dhand, R., Panayotou, G., Ruiz-Larrea, F., Thompson, A., Totty, N. F. *et al.* Phosphatidylinositol 3-kinase: structure and expression of the 110 kD catalytic subunit. Cell, *70:* 419–429, 1992.
17. Redon, R., Muller, D., Caulee, K., Wanherdrick, K., Abecassis, J., and du Manoir, S. A simple specific pattern of chromosomal aberrations at early stages of head and neck squamous cell carcinomas: *PIK3CA* but not *p63* gene as a likely target of 3q26-qter gains. Cancer Res., *61:* 4122–4129, 2001.
18. Stroschein, S. L., Wang, W., Zhou, S., Zhou, Q., and Luo, K. Negative feedback regulation of TGF-β signaling by the SnoN oncoprotein. Science (Wash. DC), *286:* 771–774, 1999.
19. Baron, B. W., Nucifora, G., McCabe, N., Espinosa, R., III, Le Beau, M. M., and McKeithan, T. W. Identification of the gene associated with the recurring chromosomal translocations t(3;14)(q27;q32) and t(3;22)(q27;q11) in B-cell lymphomas. Proc. Natl. Acad. Sci. USA, *90:* 5262–5266, 1993.
20. Feng, J., Funk, W. D., Wang, S. S., Weinrich, S. L., Avilion, A. A., Chiu, C. P., Adams, R. R., Chang, E., Allsopp, R. C., Yu, J., *et al.* The RNA component of human telomerase. Science (Wash. DC), *269:* 1236–1241, 1995.

Genomic Copy Number Analysis of Non-small Cell Lung Cancer Using Array Comparative Genomic Hybridization: Implications of the Phosphatidylinositol 3-Kinase Pathway

Pierre P. Massion, Wen-Lin Kuo, David Stokoe, et al.

Cancer Res 2002;62:3636-3640.